Journal of Hazardous Materials 163 (2009) 1165–1172

Contents lists available at ScienceDirect

Journal of Hazardous Materials

journal homepage: www.elsevier.com/locate/jhazmat

Photocatalytic decomposition of acephate in irradiated TiO_2 suspensions

ShiTong Han, Jing Li, HaiLing Xi*, DaNian Xu, Yanjun Zuo, JianHong Zhang

Research Institute of Chemical Defence, Beijing 102205, China

ARTICLE INFO

Article history:
Received 24 November 2007
Received in revised form 17 July 2008
Accepted 17 July 2008
Available online 25 July 2008

Keywords:
O,S-Dimethyl acetyl phosphoramidothioate
TiO_2
Photocatalysis
Mechanism

ABSTRACT

In the present study, the photocatalytic degradation of acephate (*O,S*-dimethyl acetyl phosphoramidothioate ($(CH_3O)(CH_3S)P(O)NHCOCH_3$)) in aqueous TiO_2 suspensions is extensively investigated, pertaining to the concentration of photocatalyst and substrate on degradation rate of acephate. It is found that the acephate can be degradated and mineralized. The high-degradation rate is obtained with 4 g/L concentration of TiO_2. Moreover, Langmuir–Hinshelowood rate expression is employed for the degradation of acephate with adsorption constant and rate constant, i.e., 2.0 L/mmol and 0.6 mmol/(min L), respectively. The main target is to identify the products by a number of analytical techniques, such as HPLC, IC, ESR and GC–MS. Under acidic condition, the primary products are phosphorothioic acid, *O,O′,S*-trimethyl ester ($CH_3O(CH_3S)P(O)OCH_3$) and phosphoramidothioic acid, *O,S*-dimethyl ester ($CH_3O(CH_3S)P(O)NH_2$), etc. It indicates that the decomposition of acephate begin from the destruction of C–N and P–N bonds. Subsequently, the P–S, P–O, P–C bonds may be oxidized gradually or simultaneously, and the final products such as CO_2, H_3PO_4, were formed. About 100% sulfur atoms are transformed into SO_4^{2-} in 180 min, however; only 3% nitrogen atoms and 2% phosphorus atoms were transformed into NO_3^- and PO_4^{3-}.

© 2008 Elsevier B.V. All rights reserved.

1. Introduction

Organophosphorous pesticide pollutant of waste water is a common problem around the world, and leads to considerable research interests [1–3]. Organophosphorous compounds (OPCs) are organic pollutants and extensively used as insecticides since they are known to inhibit acetylcholinesterase. Most of them are highly toxic to human beings and mammals. However, due to their high-chemical stability and toxicity, OPCs resist to natural decomposition and biodegradation. Moreover, owing to high polarity and dissolution capacity, they can easily penetrate into the soil and transfer to other places [4–10]. It is the important need of time to eliminate the OPCs' pollutions. There are several methods to remove OPCs from water but each method has its shortcomings. Chemical oxidation is expensive and cannot transform OPCs into minerals completely and leads to the contamination of water with other toxic pollutants. Microorganism is prone to poisoning in biodegradation technology for OPCs decomposition [1–4]. Recently, Photocatalytic oxidation has attracted increasing attention as an advanced oxidation process used to remove organic pollutants from water [5–12]. Many references have reported that some organophosphorous pesticides (containing P=S and P–S groups), such as methamidophos [5–8], malathion [1,5,11], parathion [3,10], etc., can be degradated rapidly and non-selectively in an illuminated suspension of TiO_2. The structure of these organophosphorous pesticides is presented in Fig. 1.

Malato et al. [6] studied methamidophos decomposition on P25 under sunlight and found that it is very hard to decompose. Only HCOOH and methyl phosphoric acid were detected. The authors considered that this reaction mechanism was analogous with photocatalytic oxidation of DMMP [4]. Doong and Chang [5] studied the degradation of organophosphorous pesticides by photoassisted titanium dioxide and found that the decomposition efficiency increased in the order: phorate($(C_2H_5O)_2P(S)(SCH_2SC_2H_5)$) > methamidophos($CH_3O(CH_3S)P(O)NH$) > malathion($(CH_3O)_2P(S)(SCH(CH_2C(O)C_2H_5)C(O)C_2H_5)$). They thought that this result was attributed to low-bond energy of P–S and C–S bonds. Xu et al. [7] also studied the photocatalytic degradation of methamidophos under pH 7 and found that the methamidophos can be removed but mineralization rate was low for some stable intermediates formed, such as methylphosphonic acid, etc. They also detected NO_3^-, NH_4^+, SO_4^{2-} and PO_4^{3-} concentrations by IC and found that the concentration of NH_4^+ was far more than that of NO_3^-. In addition, N–P bond was easily broken, and N atoms were mineralized completely in 80 min. Finally, CH_3SSCH_3 and $CH_3S(O)_2SCH_3$ were analyzed by GC–MS. Zhang et al. [8] researched on photocatalytic degradation of methamidophos by UV irradiation in the presence

* Corresponding author.
E-mail address: Honstrong@hotmail.com (H. Xi).

0304-3894/$ – see front matter © 2008 Elsevier B.V. All rights reserved.
doi:10.1016/j.jhazmat.2008.07.077

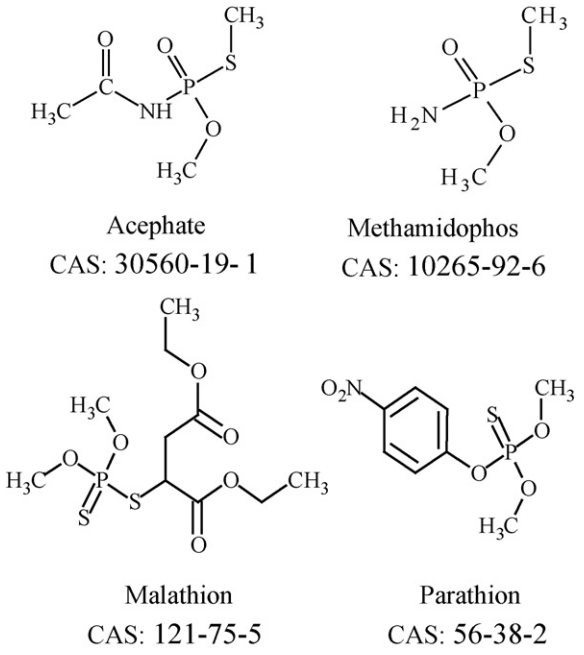

Fig. 1. The structure of acephate, methamidophos, malathion and parathion.

of nano-TiO_2 and explored the optimum TiO_2 reaction condition. A good selectivity was gained with 0.4 g/L at pH < 2 or pH > 12. The relationship between the initial degradation rate and initial concentration of the organic substrate for heterogeneous photocatalytic degradation has been described by Langmuir–Hinshelwood (L–H). The rate constant and the adsorption equilibrium constant were calculated to be 0.0027 mmol/(min L) and 2.02 L/mmol, respectively. Moctezuma et al. [10] explored particularly the reaction process of photocatalytic decomposition of methyl parathion by several analytic methods. He found that the P–S bond of methyl parathion was oxidized firstly and formed methyl paraoxon. He also found that the mineralization of methyl paraoxon was accelerated under the acidity condition. Kralj et al. [11] compared the photocatalysis of malathion, malaoxon, etc., and found sulfur in P=S and P=S groups were easily oxidized, while P was mineralized slowly. They also found that the some more toxic compounds were formed. However, these references are almost concerned about the mineralization processes of the single functional group, such as P=O, P=S, etc. In reality, most of the pesticides are consisted of many kinds of chemical bonds, which could severely influence each other during OPCs decomposes.

Acephate [13–15] ($(CH_3O)(CH_3S)P(O)NHCOCH_3$), containing P–S, P–N and P–O, etc., groups have broad-spectrum organophosphorous insecticide, which is widely used on a variety of field, fruit and vegetable crops in food handling establishments, on ornamental plants both in greenhouse and outdoors. Compared with its homologous methamidophos, acephate is less toxic and can be decomposed by biodegradation. However, acetylcholinesterase can also be inhibited strongly by contacting and chewing about of poisoned plants. It is easily removed by water in soil and remains unchanged in the soil for a long time. Its half-life in the soil ranges from 1.5 to 13 days, according to the soil properties and environmental conditions.

Only limited published work has been found about the degradation of acephate in aqueous solution by UV irradiation in the presence of TiO_2. Rahman et al. [15] had studied the influence of such reaction conditions as TiO_2 photocatalyst type, initial pH of solution, initial concentration of substrate and photocatalyst, etc. It was found that the acephate could be transformed to CO_2 and the high-degradation rate was obtained using Degussa P25 with 3 g/L at pH 3. Adding some oxidation agents, such as H_2O_2 and $KBrO_3$ into suspension can accelerate the degradation rate, but excess of these oxidation agents were required to degrade OPCs completely. The primary intermediates are (1-hydroxy-ethyl)-thiophosphoramidic acid *O*,*S*-dimethyl ester, (1-hydroxy-ethyl)thiophosphoramidic acid monomethyl ester and (1-hydroxy-ethyl)-thiophosphoramidic acid *S*-methyl ester. They postulated that these products were formed by the reaction of acephate with *OH. However, this research focused on the effects of experimental parameters on the decomposition rate of acephate. The more fundamental aspects of reaction kinetics and the mechanisms of acephate oxidation into CO_2 and H_2O were not studied. Investigations of the pathway of photocatalytic acephate in detail are still necessary to explore the photocatalytic process and decrease the formation of harmful products. Additionally, photocatalytic degradation of mixed sulfur–nitrogen functionalized organics has hardly been reported in detail yet. Research with such compounds presents interesting features [16].

In this paper, we utilize nano-TiO_2 to decompose acephate by photocatalysis, and investigate the influence of substrate and catalyst concentration on acephate decomposition. Langmuir–Hinshelwood equation with competitive adsorption of substrate and oxygen on the same type of catalytic sites is employed. The adsorption equilibrium constant and rate constant were also analyzed. We also detect the active radicals and intermediate products by electron spin resonance (ESR), HPLC and GC–MS. The mineralization processes of different elements were considered and the preferred decomposed pathways of chemical bonds were introduced. A detail reaction mechanism is also suggested according to the products. To the best of our knowledge, this is the first comprehensive study to provide detail insights on the acephate degradation reaction pathways by photocatalysis.

2. Experimental details

2.1. Materials

TiO_2 powder (100% anatase, particle size 20–30 nm, surface area 100 m^2/g) was donated by Taixin Nanometer Material Company (Jiangsu Province, China). Acephate (>98% pure) was supplied by Aldrich and used without further purification. Aqueous solutions were prepared from distilled water from all-glass distillation apparatus. HMDS (hexamethyldisilazane, CAS: 999-97-3) was used as the derivatization reagent and purchased from Supelco. The spin trap DMPO (5,5-dimethyl-1-pyrroline-*N*-oxide, CAS: 3317-61-1) was purchased from Sigma. Oxygen (99.9%) was supplied by Beifenhaipu Gas Company (Beijing, China). Other reagents were analytic grade quality and all reagents were used as received unless noted otherwise.

2.2. Instrumentations

2.2.1. HPLC

HPLC analyses were performed on a Varian-5000A instrument equipped with a Spectra 100 UV–vis detector and a stainless ODS C18 column (4.6 mm i.d. × 250 mm). The mobile phase was a mixture of acetonitrile and water (95:5, v/v). The eluent was delivered at a rate of 1 mL/min and the wavelength of detection was 220 nm. The injection volume was 10 μL.

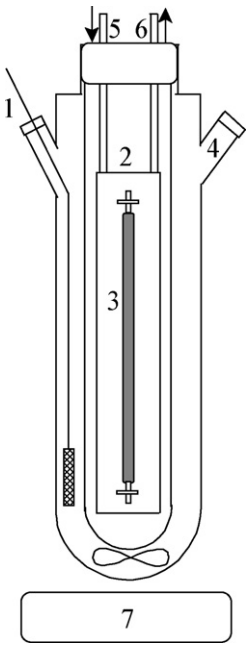

Fig. 2. The structure of the NDC-3 photocatalytic reactor.

2.2.2. IC

Quantification of inorganic anions was performed on a ZIP-3 ion chromatograph (Qingdao Analysis Instrumental Company, Shandong Province, China), which consisted of a conductivity detector and an YSA anion column. The eluent, injected 20 μL one shot, was the mixture of 3×10^{-3} mol/L $NaHCO_3$ and 2.4×10^{-3} mol/L Na_2CO_3, with a flow rate of 1 mL/min.

2.2.3. GC–MS

The products of acephate destruction in the aqueous solutions were detected by GC–MS system (HP 6890 GC-5972 MSD, with a HP-5 column 0.25 mm × 0.1 μm × 30 m) with electron impact. The chromatographic temperature programmer for GC–MS was as follows: start at 60 °C, increase to 280 °C with a gradient of 10 °C/min. Temperature of the injector and transfer line were set to 200 and 250 °C, respectively.

2.2.4. ESR

The electron spin resonance signals of radicals spin trapped by DMPO were detected on a Brucker ESP 300E spectrometer, the irradiation source was a Quanta-Ray Nd:YAG pulsed laser system (λ = 355 nm, 10 Hz). The settings for ESR spectrometer were: center field = 3486.70 G; sweep width = 100.0 G; microwave frequency = 9.82 GHz; and power = 5.05 mW [17].

2.3. General photocatalysis procedure

TiO_2 was added to 500 mL distilled water. The solution was agitated in an ultrasonic bath for 30 min under dark to ensure thorough mixing. The solution was saturated with oxygen prior to photocatalysis. Then, 500 mL suspension was poured into the reactor and vigorous stirring started. A definite amount of acephate was added at the last to minimize hydrolysis before photocatalysis. The UV lamp was turned on finally.

Magnetically stirred reaction mixtures in Pyrex tubes were irradiated in a NDC-3 photocatalytic reactor [18] (University of Nanjing, Jiangsu Province, China) presented in Fig. 2. The detail structures of the reactor were described as follows. The volume of cylindrical photoreactor was 500 mL. A high-intensity medium pressure 500 W UV lamp with max emission wavelength of 365 nm, made by Shanghai Yaming lighting Co., Ltd. and hosted in the middle of a water cooled pyrex jacket (cut-off wavelength 320 nm < λ < 450 nm), was used to carry out the reaction at temperature 28 ± 1 °C. Oxygen sparged at a rate of 500 cm^3/min, which was helpful for the suspension agitation and preventing TiO_2 from deposition during the photocatalytic experiments. This flow rate was high enough to eliminate the influence of the flow rate on the decomposition rate of acephate. The pH measurements were conducted on an Orion pH meter (model EA720). The initial pH of slurry was adjusted by HCl. The sample (5.0 mL) was taken at various time intervals and the TiO_2 was removed from the sample by 0.45 μm filtration. The filters were rinsed twice with 5 mL water to give a total volume of 15 mL solution.

2.4. Analysis of reaction products

2.4.1. Carbon dioxide

The reactive gas was passed through the reaction vessel into a saturated solution of $Ca(OH)_2$. The carbon dioxide produced during photocatalysis was trapped as solid $CaCO_3$.

2.4.2. Identification of products

2.4.2.1. Intermediate products. In order to detect the intermediate products, 500 mL aqueous solution with TiO_2 and acephate, which had been irradiated for 40 min, was filtered and extracted with 100 mL dichloromethane. Then, the organic phase was vaporized under reduced pressure to give a 5 mL residual mixture, which was subsequently dried by anhydrous sodium sulfate overnight, and analyzed by GC–MS. The rest of the solvent was also removed under reduced pressure to be condensed into a nearly dry mixture, which was derivatized by 5 mL 50% HDMS and kept in anhydrous sodium sulfate overnight. The derivants were detected by GC–MS finally [8].

Mass spectra of products were searched in the NIST 98 library and the Wiley Registry of Mass Spectral Data (7th edition). The spectra were assigned to the corresponding products if they had at least 90% similarity to the relative library spectra.

2.4.2.2. Inorganic anions. The determination of NO_3^-, PO_4^{3-} and SO_4^{2-} was performed by ion chromatography (ZIP-3 ion chromatograph). The necessary calibrations were done for measuring the concentration of ions.

2.4.2.3. Active radical species. ESR experiments had commonly been used to confirm the production of *OH radicals in the photocatalytic reaction. The characteristic ESR signal of DMPO–OH was four peaks with an intensity ratio of 1:2:2:1.

3. Results and discussion

3.1. The influence of TiO_2 concentration on acephate degradation

It is obvious that the conversion of acephate increases with time under all our experimental conditions in Fig. 3. The result shows that only about 10% acephate conversion (define as one minus the ratio of real-time concentration of acephate to the initial concentration of acephate) has been obtained after 60 min without TiO_2 or without UV. It suggests that both UV light and TiO_2 are necessary to oxide acephate and the hydrolysis of acephate can be ignored. It agrees with the previous research results that it is hard for acephate to be hydrolyzed in nature [13,15].

The influence of catalyst concentration on the acephate degradation is investigated with different concentrations of TiO_2 varying from 1 to 10 g/L. As soon as the mercury lamp turns on, a strong

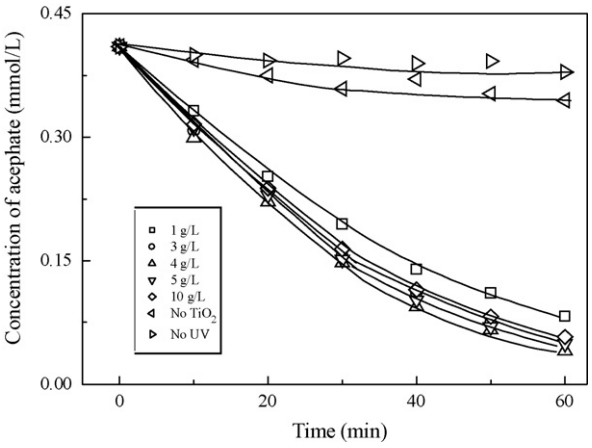

Fig. 3. Influence of TiO_2 concentration on the degradation of acephate.

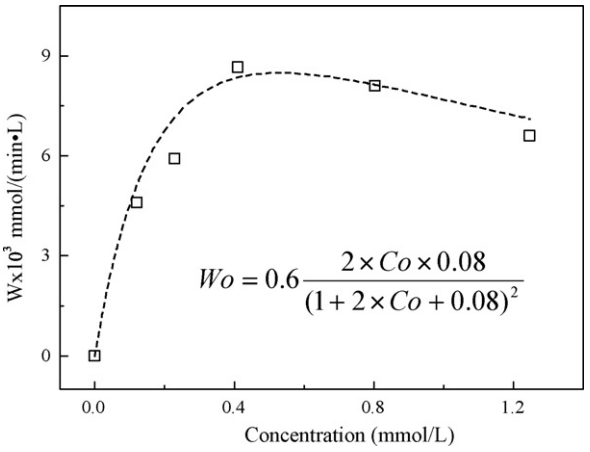

Fig. 5. Approximation of initial rates of acephate oxidation by one site Langmuir–Hinshelwood model.

enhancement of acephate decomposition is obtained in the presence of TiO_2 as expected. The highest degradation rate is observed at 4 g/L. This result can be expounded that the ultraviolet light can be penetrated into suspension easily in low-TiO_2 concentration, while, with the increase of TiO_2 concentration, ultraviolet light would be scattered and an insufficient ultraviolet light is adsorbed [8,15].

3.2. The effects of substrate concentration on acephate degradation

Acephate is stable in an acidic medium, because it is difficult to be hydrolyzed [13]. However, it has found that the highest decomposition rate of acephate is obtained when pH is around 3.7 in our previous study. It agrees with the results of Rahman's research [17].

The relationship of concentration of acephate ranging from 22 to 228 mg/L with the reaction time at pH 3.7 is shown in Fig. 4. It is found that the acephate is almost decomposed completely in 30 min under 22 mg/L. When the concentration of acephate increases from 22 to 75 mg/L, the half-life varies from 18 to 25 min. However, the conversion of acephate is very low, when the concentration of acephate reaches between 147 and 228 mg/L. Although a further increase of the substrate concentration leads to the reduction of degradation rate and the photocatalyst is not poisoned. O'Shea et al. [4] investigated the degradation of DMMP ($(CH_3O)_2P(O)CH_3$) by photocatalysis under acidic condition. The conversion of DMMP, with concentration 0.18 mg/L, was less than

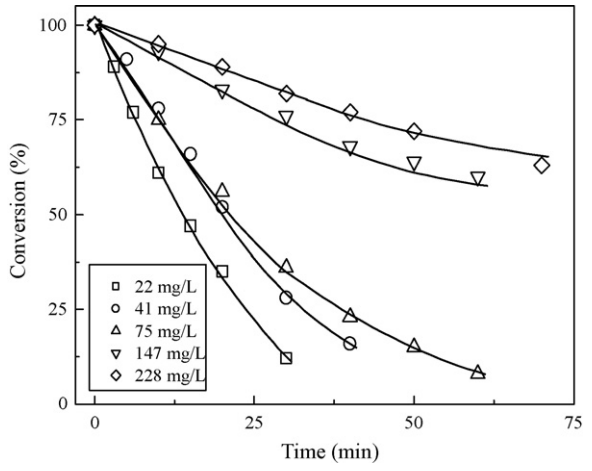

Fig. 4. Influence of substrate concentration on the degradation of acephate.

15% in 120 min. They considered that the surface of TiO_2 would hold an amount of positive charge to repulse the adsorption of DMMP, when the solvent pH was less than 6.6. However, the conversion of acephate is always fast under acidic condition in this work. So, it is suggested that the adsorption of acephate on TiO_2 does not affect the decomposition reaction seriously.

It is observed that the concentration curves in Fig. 4 follow the first order kinetics. However, when the initial concentration of substrate is 228 mg/L, the concentration versus time curves fit well to zero order dependence. Program Excel is used to calculate the initial reaction rate of acephate and the calculation is carried out using initial three to five points, which is suitable to draw a straight line [8,9]. The dependence of the initial rate of acephate on the initial concentration is studied and shown in Fig. 5. It is shown in Fig. 5 that the reaction rate increases with the substrate concentration in the range of 22–75 mg/L and the adverse result is obtained when the substrate concentration is more than 75 mg/L. It is clearly shown in Fig. 5 that the highest reaction rate is obtained at 75 mg/L acephate concentration. This result suggests that the insufficient supply of oxygen and surface adsorption sites leads to the rate decrease at high-substrate concentration. The acephate reaction behavior is similar to the degradation of other OPCs, such as: DMMP [4,10], TEP [10], TMP [10], etc., which kinetic rule had been characterized by L–H model.

So, the Langmuir–Hinshelwood equation with competitive adsorption of substrate and oxygen on the same type of catalytic sites was applied to describe the photocatalytic degradation kinetics of acephate [9]:

$$W_0 = K_p \frac{K_{op} C_0 K_{O_2} C_{O_2}}{(1 + K_{op} C_0 + K_{O_2} C_{O_2})^2}$$

where W_0 is the initial rate, K_{op} and K_{O_2} are adsorption constant of acephate and oxygen, K_p is the reaction rate constant, C_{O_2} is the oxygen concentration, and C_0 is the initial concentration of acephate. Due to the similarity of reactor between the above reference and this paper, $K_{O_2} \times C_{O_2}$ is a constant value 0.08, because all the experiments are carried out at room temperature and the concentration of dissolved oxygen is the same between our experiments and reference [9].

Fig. 5 also shows how L–H equation approximates the experimental points. Approximation by L–H equation can be used to calculate adsorption constants and rate constant for acephate. Table 1 shows these data.

The rate constant K_p and the adsorption equilibrium constant K_{op} are calculated to be 0.6 mmol/(min L) and 2.0 L/mmol. The value

Table 1
Kinetic parameters of L–H model

Compound	Acephate
K_p (mmol/(min L))	0.6
K_p (mmol/(min L))	2.0
$K_{O_2} \times C_{O_2}$	0.08

of the latter is coincident with the adsorption equilibrium constant of mineralization of methamidophos, the acephate homologous [8], but it is smaller than that of DMMP, which is about 790 L/mmol [4].

Actually, adsorption of reagents on the photocatalyst surface is considered to be critical for the reaction rate in common photocatalytic reaction [4,9–11]. It is confused that the acephate with a weak capacity of adsorption on TiO_2 is gained a quickly decomposed rate under acidic condition. We believed the following reason could explain the contradiction.

Firstly, acephate would be protonated into $(CH_3O)(CH_3S)P(O)NH_2{}^+COCH_3$. For example, Yang et al. [20,21] investigated oxidative detoxification of phosphonothiolates and found N was strongly protonated under acid solution. In addition, Vorontsov et al. [22] found that the amino group of BAET ($C_4H_9NHCH_2CH_2SH$) at pH value was less than $pK_a \sim 11$ to form $C_4H_9NH_2{}^+CH_2CH_2SH$ in dark. Moreover, the surface of TiO_2 particles is completely hydroxylated and has zero overall charge at pH ≈ 6.6. With the fall of pH value, the number of protonated sites increases, as does the overall positive charge on the particle [4,9]. So, a highly protonated surface would exclude the amine ion by electrostatic interaction and lead to a weak adsorption of acephate onto TiO_2 surface. Rahman et al. [15] also studied the adsorption of acephate on TiO_2 at different pH values and found the adsorption of acephate could be ignored under acidic condition. The similar reaction behavior has been reported in methamidophos degradation [8]. Additionally, some references also showed phosphorus atoms in OPCs were easily excluded under acidic condition.

Secondly, it is usually believed that the reaction of the *OH radical with OPCs is the control step in the photocatalysis degradation reaction [3–15]. The *OH radical, without enough long life time, could merely move the surface of photocatalyst. But the acephate couldnot be adsorbed at the surface of TiO_2. So it is puzzling how the reaction occurred between the *OH radical with protonated acephate. Recently, some investigations have indicated that hydroxyl-like chemistry may occur at or near the surface of the catalyst. Moctezuma et al. [10] explored particularly the reaction process of photocatalytic decomposition of methyl parathion. It was found that the fast mineralization rate of methyl paraoxon was gained under the acidity condition. The possible reason was hydroxyl-like chemistry may occurred near the surface of the catalyst, but it may had less rigorous requirements for specific adsorption modes or sites of adsorption than a classical electron transfer between a substrate and TiO_2 surface. Additionally, Kim and Choi [19] also investigated the kinetics and mechanisms of photocatalytic degradation $(CH_3)_nNH^+{}_{4-n}$ $(0 \le n \le 4)$ and considered that the photocatalytic oxidation of $(CH_3)_4N^+$ occurred in the solution bulk by free OH radicals under acidic condition, not at the surface TiO_2.

Although the decomposed reaction of acephate is different from conventional photocatalytic reactions which need specific adsorption modes or sites. The L–H model could still be employed to describe the kinetic rule. It suggests that the electrons excited by UV light may transfer and react at some places relatively far away from the surface of TiO_2, and the reactions mainly depend on the kinds of substrate and pH under this condition.

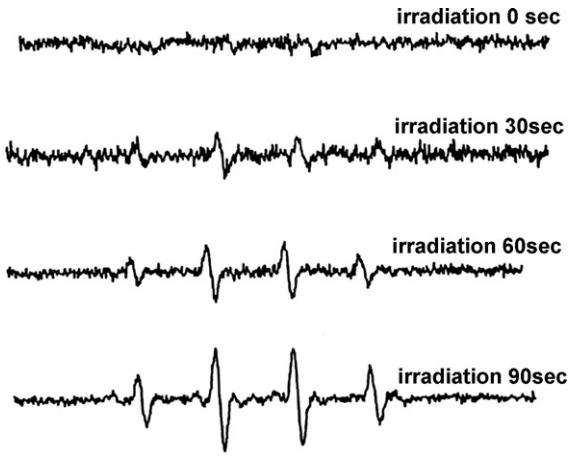

Fig. 6. The hydroxyl radical EPR spectra of acephate/TiO_2/DMPO system under UV irradiation acephate: 4×10^{-4} mol/L; TiO_2: 4 g/L and DMPO: 0.4 mol/L.

3.3. Detection of *OH radicals by ESR during in situ UV irradiation

It is critical to understand the reactive processes and pathways by detected active radicals under UV irradiation. *OH is considered as the main oxidizing agents in photocatalysis. The electron spin trapping technique is an effective method in identification of active radicals. In this work, DMPO is chosen as the scavenger of OH radicals. The result that no signals are detected without irradiation is shown in Fig. 6. However, the other experiments, detected with irradiation at different time, exhibit a fourfold peak with the intensity ratio 1:2:2:1 under in situ UV pulsed laser (λ = 355 nm). This is a typical and characteristic EPR signal of DMPO–OH adduct [17]. The change of signal intensity of hydroxyl radical at different reaction times under UV irradiation is shown in Fig. 6. It is found that the signal intensity of hydroxyl radical increases with reaction time.

3.4. Products study

The properties of intermediate and mineralization products are an important aspect to research photocatalytic technique to clean up contaminated water in the practical applications. It was essential to ascertain, on the basis of the experimentally identified intermediate species, a suitable reaction pathway for the degradation of acephate. Table 2 listed the main products detected during photocatalytic oxidation of acephate over TiO_2.

Carbon dioxide is detected by solid $CaCO_3$. The main products are phosphorothioic acid, *O,O′,S*-trimethyl ester and phosphoramidothioic acid, *O,S*-dimethyl ester, which are formed by P–N bond broken. The other intermediates are formed by the cleavage of P–S bond. In conclusion, the decomposition of acephate starts from the destruction of C–N and P–N bonds. Subsequently, the P–O, P–S, P–C bonds may be oxidized gradually or simultaneously, then, the final products, such as, CO_2, H_3PO_4, are formed.

The changes of sulfate concentration, nitrate concentration, phosphate concentration and pH during photocatalytic degradation of acephate are shown in Fig. 7. $NO_3{}^-$, $SO_4{}^{2-}$ and $PO_4{}^{3-}$ are the main mineralization products. The concentration of all these three kinds of inorganic ions increases with the reaction time. Almost the total sulfur atom is transformed into $SO_4{}^{2-}$ in 180 min. This result implies that the main mineralization pathway of acephate degradation is gained via the elimination of P–S bond. However, only 3% nitrogen atoms and 2% phosphorus atoms are transformed into the inorganic ions and indicated that the oxidation of N and P atoms is inhibited. These results are consistent with the results

Table 2
List of byproducts detected during photocatalytic oxidation of acephate over TiO_2 at 28 °C

Name of the compound	Structural formula	CAS RN	Identification based on	Remarks
O,S-Dimethyl acetyl phosphoramidothioate	$(CH_3O)(CH_3S)P(O)NHCOCH_3$	30560-19-1	GC–MS	Target
Phosphoramidothioic acid, *O,S*-trimethyl ester	$CH_3O(CH_3S)P(O)NH_2$	10265-92-6	GC–MS	Intermediate
Phosphorothioic acid, *O,O′,S*-dimethyl ester[a]	$CH_3O(CH_3S)P(O)OCH_3$	152-20-5	GC–MS	Intermediate
Monomethyl phosphate[a]	$CH_3O(HO)P(O)OH$	812-00-0	GC–MS	Intermediate
Phosphorous-acid[a]	$P(OH)_3$	10294-56-1	GC–MS	Intermediate
Methyl methanethiosulfonate	$CH_3S(O)_2SCH_3$	2949-92-0	GC–MS	Intermediate
Ethanedioic acid[a]	$(COOH)_2$	144-62-7	GC–MS	Intermediate
Phosphoric acid[a]	H_3PO_4	7664-38-2	GC–MS	Final product
Carbon dioxide	CO_2	–	$CaCO_3$	Final product
Sulphate	SO_4^{2-}	–	IC	Final product
Nitrate	NO_3^-	–	IC	Final product
Phosphate	PO_4^{3-}	–	IC	Final product

[a] By derivated with HDMS.

given by GC–MS. It shows that pH value varies from 3.7 in the beginning of reaction to 2.4 at the end of the reaction, indicating some acidic products formed. According to these results, acephate could be removed quickly under our experimental condition, and the decomposition of acephate has distinct selectivity, while, acephate is mineralized partially.

Based on the results aforementioned, reaction mechanism of photocatalytic degradation acephate is presented in Fig. 8.

The photoexcitation of TiO_2 generates an electron–hole pair, creating the potential for both reduction and oxidation processes. Although many possible degradation pathways can be envisioned, the formation and subsequent reactions of strong oxidizing and electrophilic *OH, generated from the oxidation of adsorbed water molecular and OH-groups by photoexcited TiO_2, are generally accepted as the predominant mineralization pathways of organic substrates in aqueous solutions [3–15]. The above-mentioned ESR results have confirmed that a large amount of *OH is formed. Although it is a traditional process of *OH generated at the surface of TiO_2, Above-mentioned results suggested the *OH could move to some distant places where the elimination reaction of protonated acephate happened.

Both the sulfur and the nitrogen in acephate are potential sites for oxidation. Only limited published work could be found on this subject. Yang [21,22] analyzed the products formed by the reaction of $(CH_3O)(CH_3)P(O)SC_2H_4N(i\text{-}C_3H_7)_2$ with peroxygen compounds *m*-chloroperoxybenzoic acid, and found that the oxidation of the sulfur atoms occurred only after the amino nitrogen was oxidized. The lower basicity of the sulfur relative to the nitrogen was probably a result of electron delocalization to the phosphoryl oxygen.

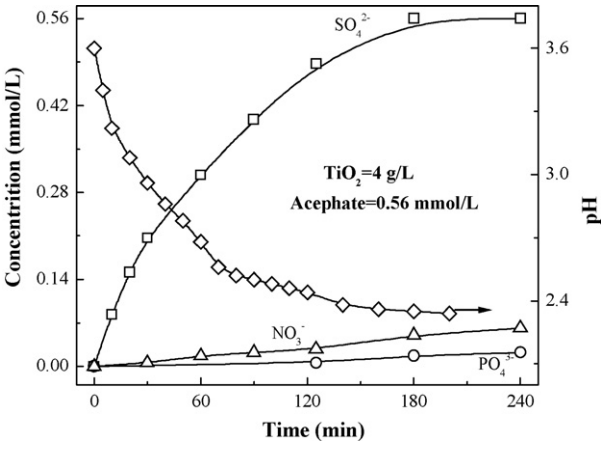

Fig. 7. Changes of sulfate concentration, nitrate concentration, phosphate concentration and pH during photocatalytic degradation of acephate.

Consistent results were found in the photocatalytic decomposition of methamidophos [8].

The C–N bond in protonated acephate favorably breaks by the electrophilic OH radicals attacked under acidic condition, and the main reaction products are $CH_3O(CH_3S)P(O)NH_2$ and CH_3COOH. Rahman also detected the main products, formed from acephate photocatalytic decomposition. They postulated the initial reaction pathway occurred between the reaction of carbonyl in acephate and *OH [15]. The differences ascribed by Rahman's result were analyzed under neutral condition. On the contrary, If $HONHC(O)CH_3$ would exist abundantly by decomposing P–N bond, it was hardly to be oxidized or reduced under acidic condition [19] and easy to be detected. However, it was not found in the reaction system. It suggests that the decomposition of C–N bond is the first step for acephate photocatalytic degradation. Although CH_3COOH was not found, its subsequent oxidization product HOOCCOOH was detected.

$CH_3O(CH_3S)P(O)NH_2$ is a kind of deadly pesticide and hard to be degradated. Some references researched the photocatalytic degradation of methamidophos ($CH_3O(CH_3S)P(O)NH_2$) under alkaline condition [5–8,13,14], but few insights about its degradation mechanism were studied under acidic condition. Although methamidophos could also be protonated under acidic condition, N–P bond would be broken by hydrolysis reaction. Vorontsov et al. [12,16] analyzed the products of photocatalytic degradation of DEPA ($(C_2H_5O)_2P(O)NH_2$) and found that the cleavage of P–N bond was the main mineralization pathway of DEPA. So, $CH_3O(CH_3S)P(O)OH$ and NH_3 would be formed in principle. The former is not found, but its subsequent oxidation product $CH_3O(HO)P(O)OH$ was detected. It is possible that $CH_3O(CH_3S)P(O)OH$ was unstable and can be oxidized or substituted easily, attributed to low-bond energy of P–S [5–8]. $CH_3O(CH_3S)P(O)(OCH_3)$ may come from the reaction of $CH_3O(CH_3S)P(O)NH_2$ and $^{\bullet}OCH_3$.

Subsequently, C atom in $CH_3O(HO)P(O)OH$ could be eliminated by an H-abstraction or addition–elimination with *OH [4,12]. Then, the mineralization product H_3PO_4 is produced. Explanatorily, at low pH, the mineralization rate of P atoms is very slow, presumably as a result of a highly protonated surface, which leads to weak adsorption of $CH_3O(HO)P(O)OH$, etc. on the surface of TiO_2. In addition, some byproducts from removed acephate, such as methamidophos, were more stable than acephate. So, the PO_4^{3-} concentration is low after a long time UV irradiation. It agreed with the result of photocatalytic degradation of DMMP [4,9,12]. $P(OH)_3$ was found first in the photocatalytic degradation of acephate and may come from the reduction of H_3PO_4.

In addition, $CH_3S(O)_2SCH_3$, formed from the rest segment of $CH_3O(CH_3S)P(O)NH_2$ oxidized by *OH, is detected here. It is likely formed by the following pathway. $^{\bullet}CH_3S$ is formed

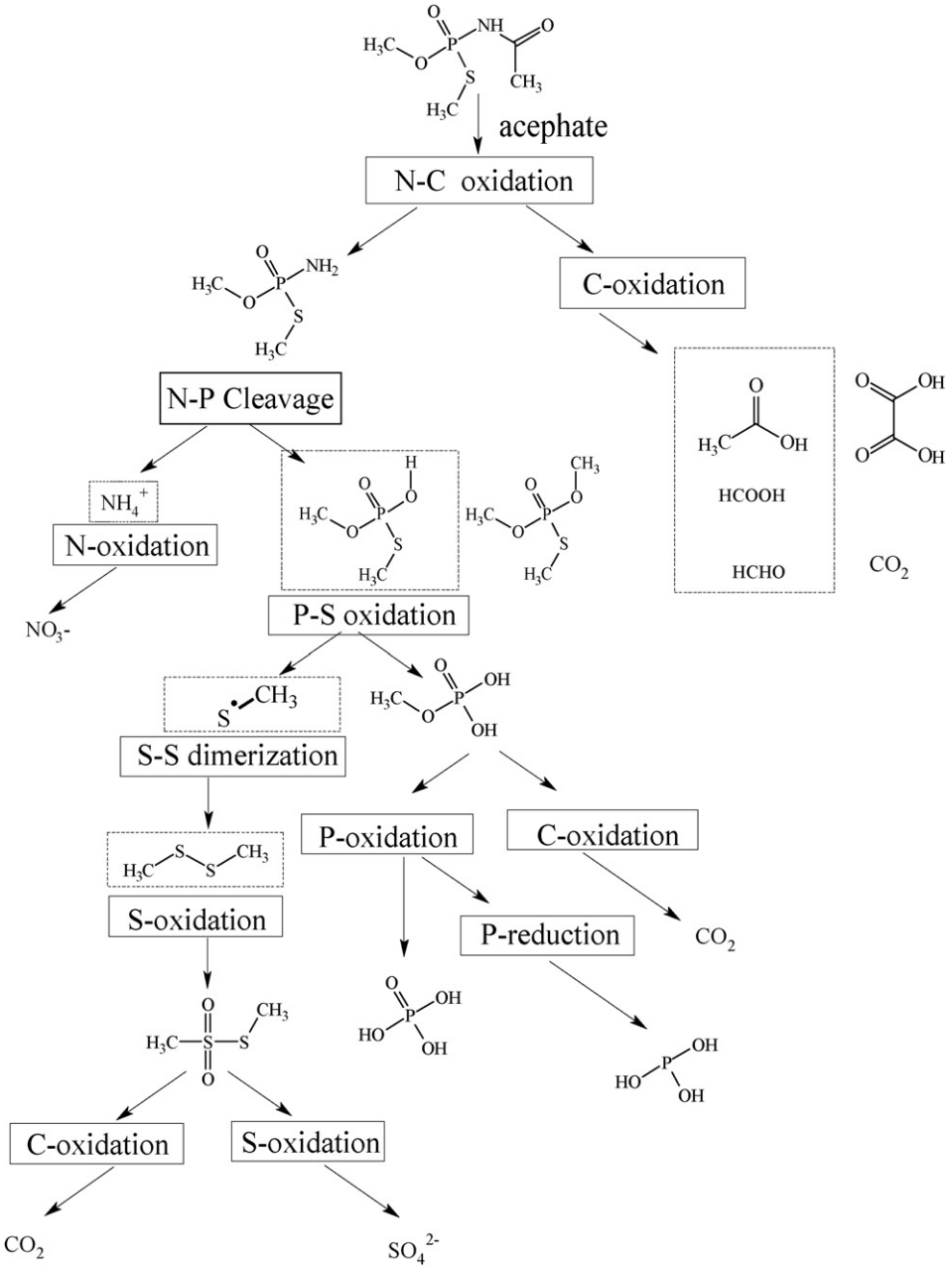

Fig. 8. Main starting routes of photocatalytic degradation of acephate. The dotted square means the possible products but cannot be measured.

from the reaction of methamidophos with *OH, the dimerization of $^{\bullet}CH_3S$ on the surface results in the formation of CH_3SSCH_3 quickly, which is oxidized further into thiosulfinate and thiosulfonate. Thiosulfonate is not stable in aqueous solution and disproportionates into starting disulfide and thiosulfonate. Vorontsov et al. [16,22] deeply investigated the degradation of 2-PECES (2-phenethyl-2-chloroethyl sulfide) in irradiated TiO_2 suspensions and found the similar reaction mechanism for $C_6H_5CH_3S(O)_2SCH_3C_6H_5$. Xu et al. [7] also detected $CH_3S(O)_2SCH_3$ during the photocatalytic degradation methamidophos. The oxidation reaction continued and $CH_3S(O)_2SCH_3$ is transferred into SO_4^{2-}. Vorontsov et al. [16] found *OH attacked primarily S of protonated BAET (2-(butylamino)ethanethiol) under acidic condition, and some amount of SO_4^{2-} was formed, from further oxidation of sulfone and sulfoxide. Attributed the low-bond energy of P–S, S atoms were transformed to SO_4^{2-} completely in 180 min.

Further, when P–N bond broke, NH_3 was removed from protoned $CH_3O(CH_3S)P(O)NH_3^+$ and transformed into NH_4^+ under acidic condition. Kim and Choi [19] introduced that the main pathways of photocatalytic decomposition nitrogen compounds would form NH_4^+ under acidic condition and it would form NO_3^- and NO_2^- at 11–12 pH value. In addition, NH_4^+ was seldom transformed to NO_3^-, NO_2^- in low pH. This explained the reason why just a small amount of NO_3^- was measured.

Finally, the carbon atom in acephate can react with *OH and be oxidized, forming final products, such as, $(COOH)_2$ and CO_2·HCOOH, HCHO, etc. are also considered to be formed, but they are easy to volatilize and could miss in the sample preparation. In a word, the reaction mechanism, given here, are primary steps. During

further deeper reaction, these above-mentioned reaction routes would intersect each other. So, the actual reaction mechanisms are severely complicated.

4. Conclusion

The photocatalytic degradation of acephate (*O*,*S*-dimethyl acetyl phosphoramidothioate) in aqueous TiO_2 suspensions is studied in detailed. It is found that the acephate can be decomposed and mineralized. The dependence of acephate conversion on the concentration of photocatalyst and substrate is investigated deeply, and the highest degradation rate observed at 4 g/L TiO_2. Langmuir–Hinshelowood rate expression is used to expound the degradation of acephate with adsorption constant and rate constant equaling to 2.0 L/mmol and 0.6 mmol/(min L), respectively. It demonstrates that the adsorption is not a key factor for decomposition of acephate and suggests that the reaction between the acephate with the $^{*}OH$ radical occur near the surface of TiO_2, instead of at TiO_2 surface.

The main products are identified by HPLC, IC, ESR and GC–MS. The primary products are phosphorothioic acid, *O*,*O*′,*S*-trimethyl ester and phosphoramidothioic acid, *O*,*S*-dimethyl ester were detected by GC–MS and derivated techniques, and the $^{*}OH$ radical was also detected by ESR under acidic condition. Based on the active radicals, main intermediate species and final products, the reaction mechanism of photocatalytic degradation acephate is proposed. The decomposition of acephate starts from the destruction of C–N and P–N bonds. Subsequently, the P–S, P–O, P–C bonds may be oxidized gradually or simultaneously. Later, the final products, such as, CO_2, H_3PO_4, are formed. The analytical results show that about 100% sulfur atoms are transformed into SO_4^{2-} in 180 min. Only 3% nitrogen atoms and 2% phosphorus atoms are oxidized into NO_3^-, PO_4^{3-}. It indicates that the decomposition of acephate has distinct selectivity, while acephate is mineralized partially.

Acknowledgements

The work described here is financially supported by the National Natural Science Foundation of China (Nos. 20473113). The authors appreciate the assistance of Prof. Zhao J.C.

Appendix A. Supplementary data

Supplementary data associated with this article can be found, in the online version, at doi:10.1016/j.jhazmat.2008.07.077.

References

[1] S. Chiron, A.F. Alba, A. Rodriguez, Pesticide chemical oxidation: state-of-the-art, Water Res. 34 (2000) 366–377.
[2] Jean-Marie Herrmann, Chantal Guillard, Photocatalytic degradation of pesticides in agricultural used waters, J. Acad. Sci. Paris, Seĭrie IIc, Chim.: Chem. 3 (2000) 417–422.
[3] H.D. Burrows, M. Canle, L.J.A. Santaballa, Reaction pathways and mechanisms of photodegradation of pesticides, J. Photochem. Photobiol. B: Biol. 67 (2002) 71–108.
[4] K.E. O'Shea, S. Beightol, I. Garcia, Photocatalytic decomposition of organophosphonates in irradiated TiO_2 suspensions, J. Photochem. Photobiol. A: Chem. 107 (1997) 221–226.
[5] Ruey-an Doong, Wen-huei Chang, Photoassisted titanium dioxide mediated degradation of organophosphorus pesticides by hydrogen peroxide, J. Photochem. Photobiol. A: Chem. 107 (1997) 239–244.
[6] S. Malato, J. Blanco, C. Richter, B. Milow, Solar photocatalytic mineralization of commercial pesticides: methamidophos, Chemosphere 38 (1999) 1145–1156.
[7] Yuehua Xu, Lianyan Wang, Guobang Gu, Study on photocatalytic degradation of methamidophos Shanghai, Environ. Sci. 21 (2002) 574–576.
[8] Lei Zhang, Fei Yan, Yingnan Wang, Photocatalytic degradation of methamidophos by UV irradiation in the presence of nano-TiO_2, J. Inorg. Mater. 42 (2006) 1379–1387.
[9] E.A. Kozlova, P.G. Smirniotis, A.V. Vorontsov, Comparative on photocatalytic oxidation of four organophosphorous simulants of chemical warfare agents in aqueous suspension of titanium dioxide, J. Photochem. Photobiol. A: Chem. 162 (2004) 503–511.
[10] E. Moctezuma, E. Leyva, G. Palestino, Photocatalytic degradation of methyl parathion: reaction pathway and intermediate reaction products, J. Photochem. Photobiol. A: Chem. 186 (2006) 71–84.
[11] M.B. Kralj, U. Černigoj, M. Franko, Comparison of photocatalysis and photolysis of malathion, isomalathion, malaoxon, and commercial malathion-products and toxicity studies, Water Res. 41 (2007) 4504–4514.
[12] A.V. Vorontsov, L. Davydov, E.P. Reddy, Routes of photocatalytic destruction of chemical warfare agents simulants, N. J. Chem. 26 (2002) 732–744.
[13] A.D. St-Amand, L. Girard, Determination of acephate and its degradation product methamidophos in soil and water by solid-phase extraction and GC–MS, J. Environ. Anal. Chem. 84 (2004) 739–748.
[14] P.E. Athanasopoulos, C. Pappas, N.V. Kyriakids, Degradation of methamidophos on soultanina grapes on the vines and during refrigerated storage, Food Chem. 91 (2005) 235–240.
[15] M.A. Rahman, M. Qamar, M. Muneer, Semiconductor mediated photocatalysed degradation of a pesticide derivative, acephate in aqueous suspension of titanium dioxide, J. Adv. Oxid. Technol. 9 (2006) 103–109.
[16] A.V. Vorontsov, Y.C. Chen, P.G. Smirniotis, Photocatalytic oxidation of VX simulant 2-(butylamino)ethanethiol, J. Hazard. Mater. 113 (2004) 89–95.
[17] T.X. Wu, T. Lin, J.C. Zhao, TiO_2-assisted photodegradation of dyes: photooxidation of a squarylium cyanine dye in aqueous dispersions under visible light irradiation, Environ. Sci. Technol. 33 (1999) 1379–1387.
[18] C. Hu, Y.Z. Wang, H.X. Tang, Preparation and characterization of surface bond-conjugated TiO_2–SiO_2 and photocatalysis for azo dyes, Appl. Catal. B: Environ. 30 (2001) 277–285.
[19] S.Y. Kim, W.Y. Choi, Kinetics and mechanisms of photocatalytic degradation of $(CH_3)_nNH^+_{4-n}$ $(0 \le n \le 4)$ in TiO_2 suspension: the role of OH radicals, Environ. Sci. Technol. 36 (2002) 2019–2025.
[20] Y.-C. Yang, L.L. Szafraniec, W.T. Beaudry, Oxidative detoxification of phosphonothiolates, J. Am. Chem. Soc. 112 (1990) 6621–6627.
[21] Y.-C. Yang, Chemical detoxification of nerve agent VX, Acc. Chem. Res. 32 (1999) 109–115.
[22] A.V. Vorontsov, A. Panchenko, E.V. Savinov, Photocatalytic degradation of 2-phenethyl-2-chloroethyl sulfide in liquid and gas phases, Environ. Sci. Technol. 36 (2002) 5261–5269.